Computers and Concrete, *Vol. 13, No. 3 (2014) 361-375*
DOI: http://dx.doi.org/10.12989/cac.2014.13.3.361

Nonlinear calculation of moisture transport in underground concrete

M.F. Ba[1a], C.X. Qian[*1b] and G.B.Gao[3c]

[1]*Faculty of Architectural Civil Engineering and Environment*, *Ningbo University*, *Ningbo*, *315211*, *China*
[2]*School of Materials Science and Engineering*, *Southeast University*, *Nanjing*, *211189*, *China*
[3]*Shandong Provincial Academy of Building Research*, *Jinan 250031*, *China*

(*Received June 25, 2012, Revised November 9, 2013, Accepted November 26, 2013*)

Abstract. The moisture transport in underground concrete was experimentally investigated and the nonlinear model of moisture transport considering the effects of water diffusion, hydration of cementicious materials and water permeability was proposed. The consumed moisture content by self-desiccation could be firstly calculated according to evolved hydration degree of cement and mineral admixtures. Furthermore, the finite differential method was adopted to solve the moisture transport model by linearizing the nonlinear moisture diffusion coefficient. The comparison between experimental and calculated results showed a good agreement, which indicated that the proposed moisture model could be used to predict moisture content evolution in underground concrete members with drying–wetting boundaries.

Keywords: nonlinear moisture model; underground concrete; hydration degree evolution

1. Introduction

The moisture content in concrete pores directly affects mechanical and thermal properties of concrete and even is a critical parameter for most of the degradation processes suffered by concrete (Zhang 2009, Garboczi 1996, Tariku 2010). The driven force for moisture migration mainly includes diffusion action and hydration of cement-based materials. Materials properties such as age-dependent diffusion coefficient are correlated with hydration-related parameter which is unavoidably affected by the curing condition (Khelidj 2007). That is to say, after a period of curing, the moisture inside concrete structures is the results of natural conditions. Thus prediction of moisture distributions requires a number of data on material properties and information on the microclimate in the different parts of the concrete structures (Oh 2003, Qin 2009). A large number of references are found in literatures on the investigation of distribution of relative humidity over time by diffusion in matured concrete (Nilsson 2002, Ozbolt 2010, Parrott 1995).The hydration-induced moisture changes by cement, especially by mineral admixtures in concrete, is not well

∗Corresponding author, Ph.D., E-mail: cxqian1966@126.com
[a]Ph.D., Email : bmf-1@163.com
[b]Professor, Email: cxqian1966@126.com
[c]Ph.D., Email: guibogao@163.com

http://www.techno-press.org/?journal=cac&subpage=8 ISSN: 1598-8198 (Print), 1598-818X (Online)

established even though these topics have been brought to great attention recently (Breugela 2000, Buffo-Lacarrière 2007, Fraj 2012).

Direct experimental observation of hydration-driven moisture flow is very difficult, if possible at all, therefore in this paper the model of moisture content transport was refined based on the hydration mechanism of cement and mineral admixtures in concrete. And then this model was incorporated to analyze the practical moisture content distribution in simulated underground concrete member with initial steam and water curing condition. Simultaneously, the inner distribution of temperature and relative humidity in above simulated member were also monitored and compared with the calculated results.

2. Experimental

2.1 Experimental program

2.1.1 Materials and concrete proportions

The mixtures were made with Chinese Normal Portland Cement P.I52.5. Natural sand with 2.9 fineness modulus and crushed granite rocks with 5~25 mm particles were used as fine and coarse aggregates. The used granulated blast furnace slag and fly ash was named as S95 and I grade according to China Standard. The corresponding chemical compositions of the cement, slag and fly ash were shown in Table 1 and Table 2 showed the corresponding mixture proportions.

2.1.2 Humidity and temperature testing

Prismatic specimens were cast and waterproof plywood molds with the inner size of 600 mm × 400 mm × 400 mm were used. In order to guarantee one dimensional heat and moisture transportation in underground concrete structure, inner surfaces of molds were covered with heat-insulating waterproof sheet, except one 400 mm × 400 mm face exposed to inside of tunnel and the other 400 mm × 400 mm side contacted with saturated underground soils.

During concrete casting, five digital sensors sealed with waterproof breathable cloth were

Table 1 Chemical components and physical properties for cementicious materials

Type of binder	Chemical composition (%)										Gravity (kg/m^3)
	Loss	SiO_2	Al_2O_3	Fe_2O_3	CaO	MgO	SO_3	K_2O	Na_2O	Total	
P.I 52.5 Cement	2.29	19.49	4.08	4.03	64.59	1.97	2.33	0.37	0.07	99.22	ρ_c=3145
Fly-ash	3.21	56.02	28.00	6.20	3.60	1.21	0.61	0.89	0.23	99.97	ρ_f=2550
Slag	0.03	34.35	2.35	15.20	35.38	8.54	0.12	0.32	0.63	96.92	ρ_s=2896

Table 2 Proportion of segment concrete (kg/m^3)

No	C	FA	SL	G(10-20 mm)	G (5-10 mm)	S	W	SP
FS	322	83	55	736	397	694		3.22

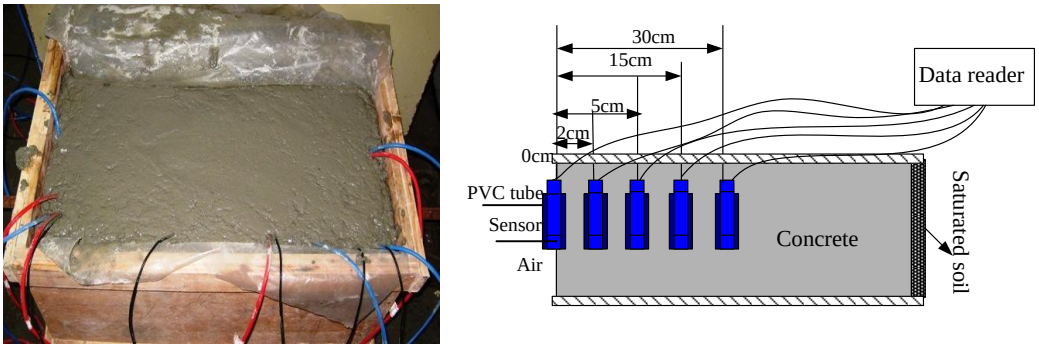

Fig.1 Practical and schematic picture of humidity testing

placed in the position of 0 cm, 2 cm, 5 cm, 15 cm and 30 cm from the exposure surface to measure the moisture and temperature of concrete. The detailed schematic testing positions and the practical specimen were shown in Fig. 1.

After cast, the specimens were directly put into the steam curing chambers and steam cured for 14 hour at 50 ± 2℃. Then specimens cured in the chamber charged with water at 20 ± 2℃ for 14 day. After then, the water was released to make one 400 mm × 400 mm side exposed to air condition and the other 400 mm × 400 mm covered with water-filled sponge in the room with 70% relative humidity at 20 ± 2℃. It was notable that the moisture and temperature data in concrete specimens were monitored since completion of cast.

2.2 Testing results of humidity and temperature

The evolution of interior relative humidity with time since concrete cast at five testing positions was shown in Fig. 2. It could be seen from Fig. 2(a) that the relative humidity inside concrete decreased quickly with the steam curing duration and then it increased to saturation state at age of 2days. After then, this state was kept until end of water curing. The distribution of relative humidity during steam curing varied significantly along the specimen depth from one exposed surface 400 mm × 400 mm. The inner the depth, the lower humidity was obtained. This could be attributed to variation of temperature distribution in corresponding depths.

Fig. 2(b) illustrated that relative humidity at the drying surface decreased to equalize with air humidity very soon once exposed to room condition. The relative humidity at depth O and A poi nt decreased quickly over time while relative humidity at inner location C and D exerted much lower decrease. It was observed that the relative humidity at location A and B is 87 ~88% at age of 200 day while that at location C and D was over 90%. Anyway, there were very obvious humidity gradients between outer and inner locations in simulated specimen, which unavoidably would induce the moisture diffusion. The temperature results at five testing locations after cast was sho wn in Fig. 3.

It could be seen from Fig. 3 that the changing tendency of temperature inside specimen was consistent with that in curing chamber and the farer location had much higher temperature as the lower release rate of hydration heat. While it was only 3 days after initial steam curing, the temperature gradients between every location began to disappear. This indicated that temperature e ffect on moisture transport in this study could be neglected.

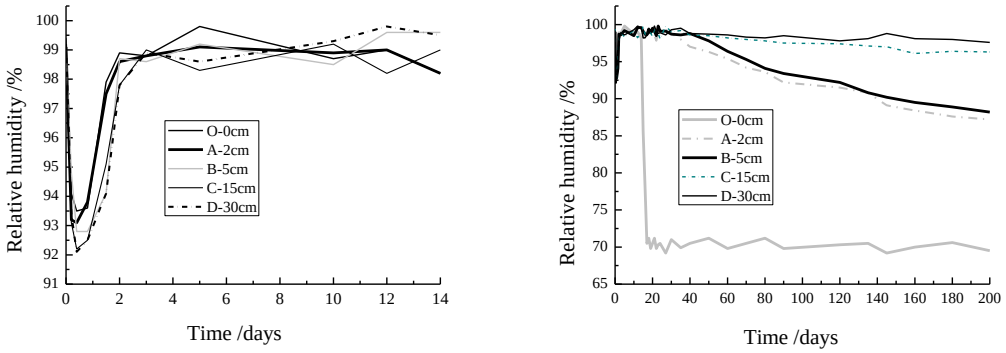

(a) Changes of RH before 14days (b) RH changes after 14days

Fig. 2 Changes of interior humidity with time in simulated segment concrete

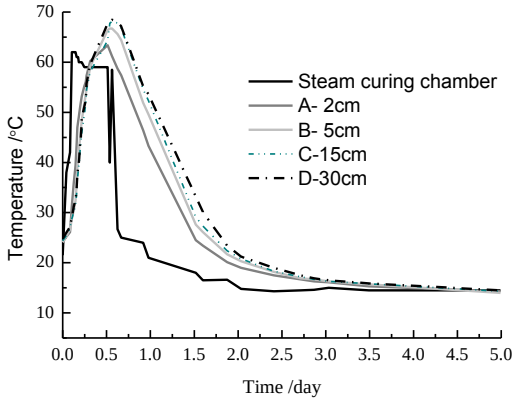

Fig. 3 Changes of temperature inside segment concrete

3. Moisture transport model of concrete with mineral admixtures

The Newton – Raphson iterative procedure, commonly used to solve nonlinear systems of equations in finite element analyses, may have two alternative forms: (a) with control of the applied load and (b) with control of the applied displacement. Following a brief review of the basic features of these two methods, their numerical implementations, in conjunction with the concrete material behaviour that was described above, are developed.

3.1 Moisture distribution model

The state of water in pore system consists of three parts: chemically bound water, physically bound water and free evaporable water. It was well known that the pores in concrete are fully or partially filled with free water and the free evaporable water can move through the capillary pores. As the variation of moisture content inside concrete is a result of moisture diffusion and self-desiccation during curing period as shown in Eq. (1)

$$\begin{cases} \dfrac{\partial w}{\partial t} = \dfrac{\partial}{\partial x}\left(D_{eff}(w) \dfrac{\partial w_d}{\partial x} \right) + \dfrac{\partial w_h}{\partial t} \\ \dfrac{dw}{dt} = \dfrac{dw_d}{dt} + \dfrac{dw_h}{dt} \\ \dfrac{\partial w_d}{\partial t} = \dfrac{\partial}{\partial x}\left(D_{eff}(w) \dfrac{\partial w_d}{\partial x} \right) \end{cases} \tag{1}$$

where w is the volume content of capillary water in per-cubic concrete (m^3/m^3), w_d and w_h is the volume content of capillary water by diffusion and hydration respectively (m^3/m^3); $D_{eff}(w)$ is the effective moisture diffusion coefficient (m^2/h).

After curing, the concrete segment was assembled inside underground. As the outer face of segment was directly contacted with saturated soil, it's very necessary to consider the effects of water permeability on moisture content under certain hydraulic pressure. Therefore the moisture content variation of assembled concrete segment can be expressed as following equation:

$$\frac{\partial w}{\partial t} = \left(\frac{\partial}{\partial x}\left(D_{eff}(w) \frac{\partial w_d}{\partial x} \right) \right) + \left(\frac{\partial}{\partial x}\left(\frac{K_p \cdot \rho_w}{\mu} \frac{\partial p}{\partial x} \right) \right) + \frac{\partial w_h}{\partial t} \tag{2}$$

where p means the hydraulic pressure of underwater tunnels (Pa) and K_p is the permeability coefficient of concrete segment (m/h).

It has been known that water seepage in concrete is nonlinear and achieves equilibrium very soon (Qian 2009). For instance the equilibrium permeable depth of concrete segment in this paper is only 12.5 mm, which only affects the location of saturated boundary condition. Therefore this study focus on only the moisture content development model in Eq. (1).

3.2 Hydration-driven water loss equation

In concrete with mineral admixtures, the decrease of evaporable water is induced by hydration action of both cement and mineral admixtures. Thus in term of the mechanism of hydration, the consumed evaporable water in concrete can be expressed as in Eq. (2)

$$w_h = (w_c \cdot m_c \cdot \alpha_c(t) + w_f \cdot m_f \cdot \alpha_f(t) + w_s \cdot m_s \cdot \alpha_s(t)) / \rho_w \tag{3}$$

where m_c , m_f and m_s are the mass of cement, fly-ash and slag in per-cubic concrete (kg/m^3) and w_c, w_f and w_s are the mass of evaporable water needed for complete hydration of per-mass cement, fly-ash and slag (kg/kg). α_c, α_f and α_s are the hydration of cement, fly-ash and slag in concrete (%)and ρ_w is the density of water at standard state (kg/m^3).

According to T.C Power's hydration model (Power 1947), w_c is determined to be 0.42, and in terms of X.Y Wang's study (Wang 2010), w_f and w_s is deduced to be 0.25 and 0.45 respectively. Therefore Eq. (3) can be adjusted as follows

$$w_h = (0.42 m_c \cdot \alpha_c(t) + 0.25 m_f \cdot \alpha_f(t) + 0.45 m_s \cdot \alpha_s(t)) / \rho_w \tag{4}$$

As it is difficult to determine the dividing point in the classical cement hydration model (Krstulovic 2000), thus the modified Knudsen's parabolic equation on hydration (Knudsen 1984)

was adopted here to calculate hydration degree of cement in concrete as shown in Eq. (5), which especially is applicable to concrete with low water-cement ratio.

$$\alpha_c(t) = \frac{\psi(t-t_0)^{1/2}}{1+\psi(t-t_0)^{1/2}} \tag{5}$$

where t_0 is the induction time of cement hydration (h), and Ψ is average value of reaction rate constant ($h^{(-1/2)}$), both of which are related to the cement components, water-cement ratio and as well as curing condition.

Previous studies on hydration kinetics of mineral admixtures had shown that the exponential decline formula in Eq. (6) and Eq. (7) could accurately represent the hydration development of fly ash and slag in concrete.

$$\alpha_f(t) = a_f - b_f \exp(-t/t_f) \tag{6}$$

$$\alpha_s(t) = a_s - b_s \exp(-t/t_s) \tag{7}$$

By combining above equations, the changing rate of consumed-moisture content by hydration can be express as

$$\frac{dw_h}{dt} = [0.42m_c \cdot (\frac{1}{2\psi(t-t_0)^{3/2}} - \frac{0.25m_f b_f}{t_f}\exp(-t/t_f) - \frac{0.45m_s b_s}{t_s}\exp(-t/t_s)]/\rho_w \tag{8}$$

3.3 Initial and boundary condition

In order to resolve the nonlinear differential equation of moisture transfer, the initial and boundary equation could be determined according to the experimental condition. During water curing duration, the inner water content at every point of specimen can be assumed to be the capillary porosity of specimen, although the initial water content of specimen equals to volume content of water in per-cubic mixing concrete as shown in following two equations.

$$w(x,t_0) = w_0 = 14.29\% \qquad 0 \le x \le 0.6m \tag{9}$$

$$w(x,t) = \phi_{cap}(t) \quad 0 \le t \le 14d \tag{10}$$

After the end of water curing, the concrete specimen was exposed to drying condition with constant 70% relative humidity at 20 ± 2℃. The measured relative humidity over drying time at the drying surface could be converted into corresponding moisture content.

As for the surface covered with water saturated soil, its volume content of moisture were suggested be porosity of concrete over age. In this study the capillary porosity of segment concrete with time could be expressed by the following equation

$$\phi_{cap} = 10.31\exp(-t/4.27) + 4.08 \tag{11}$$

3.4 Determination of related calculation parameters

3.4.1 Effective moisture diffusion coefficient of concrete

Effective moisture diffusion coefficient is much influenced by porous structure as well moisture condition of concrete (Papadakis 1999, Ye 2005). As the porous structure of specimen in this study was in nearly stable state and the temperature gradient disappeared by the end of water curing, thus only effects of self-moisture condition was considered in determination of the effective moisture diffusion coefficient. Furthermore, water evaporation is the major component of transferred moisture content, so effects of Knudsen diffusion was also taken into considered in $D_{eff}(w)$, which was shown in Eq. (12)

$$D_{eff}(w) = k_f D(w) \tag{12}$$

where $D(w)$ is moisture related coefficient and k_f is influencing factor of Knudsen diffusion，which can be defined as

$$k_f = (1-r) + \frac{r \cdot d}{3D(w,T)} \cdot \sqrt{\frac{3RT}{M_w}} \tag{13}$$

where r is water-vapor-to-total-moisture ratio, r = 1 represents complete vapor transfer and r = 0 represents transfer of liquid water; d is the average diameter of capillary pore (nm); M_w is molar mass of water (kg/mol).

Given the temperature was constant and influence factor of Knudsen was known, introducing the parameter $\eta = x/t^{1/2}$, the partial differential equation (Eq. (1)) was converted into ordinary differential equation

$$-\frac{\eta}{2} dw_d = d\left(D(w_d) \frac{dw_d}{d\eta} \right) \tag{14}$$

Integrating above equations at the interval w to w_0, it can be obtained that

$$\int_w^{w_0} -\frac{\eta}{2} dw_d = \int_w^{w_0} d\left(D(w_d) \frac{dw_d}{d\eta} \right) = \left(D(w_d) \frac{dw_d}{d\eta} \right)_{w_0=\phi_{cap}(14d)} - \left(D(w_d) \frac{dw_d}{d\eta} \right)_{w_d=w} \tag{15}$$

where

$$\left(D(w_d) \frac{dw_d}{d\eta} \right) = \left(D(w_d) \frac{dw_d}{dx} \frac{dx}{d\eta} \right) = \left(D(w_d) \sqrt{t} \frac{dw_d}{dx} \right) \tag{16}$$

As at age of 14 day, moisture content at every point of specimen was the same value, thus Eq. (15) can be simplified as

$$-\frac{1}{2}\int_{w}^{w_0}\frac{x}{\sqrt{t}}dw_d=\left(D(w)\sqrt{t}\frac{dw_d}{dx}\right)_{w_d=w} \tag{17}$$

Finally, the effective moisture diffusion coefficient can be calculated by

$$D(w)=\frac{1}{2t}\left(\left.\frac{dw_d}{dx}\right|_{w_d=w}\right)^{-1}\cdot\int_{w}^{w_0}xdw_d \tag{18}$$

It can be seen that as long as the experimental curve of water contend by diffusion (w_d) and diffusion distance was obtained, the moisture related diffusion coefficient $D(w)$ can be deduced by multiplying the reciprocal and integration value at point of w_d.

3.4.2 Experiments for determining the D(w)

Two sets of specimens (100 mm × 100 mm × 400 mm) with the same kind of lining concrete were made. They were steam-cured for 14 hours and water-cured for 14 days. Then all surfaces of one group of specimen were sealed with waterproof insulation materials and only two relative sections (100 mm×100 mm) of another group were sealed. After then the specimens were put in the curing room with 50% RH and 10 km/s wind speed at 20 ± 2℃. 90 days later the specimens were taken out and cut into thin slices along its length. Then the moisture contents of every slice

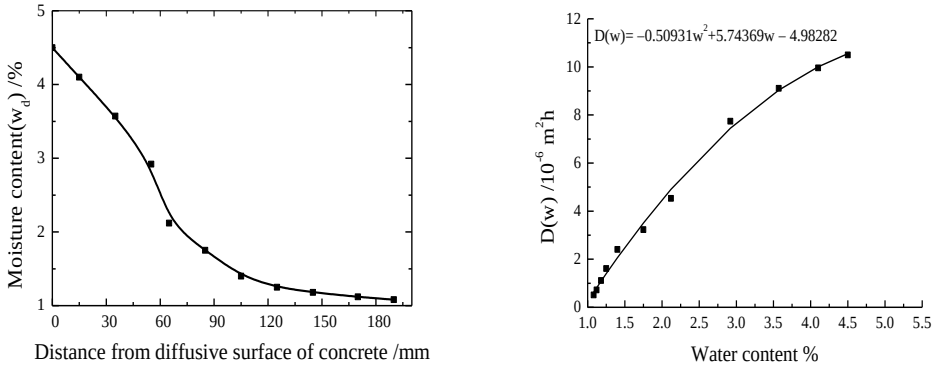

(a) Diffused moisture contents along lentgh (b) Moisture diffusivity varying with moisture content (w_d)

Fig. 4 The relation between diffusive coefficient and diffusive moisture content

Table 3 The related calculation parameters

Parameters	Symbols	Values
Influencing factor of knudsen diffusion	k_f	0.98
Average hydration rate of cement	Ψ	0.251 $h^{1/2}$
Volume content of paste in concrete specimen	A	0.30
Induction time	t_0	3 h

could be obtained. Finally the diffusive moisture content w_d at certain position equals the difference of moisture content between sealed slice and non-sealed one at the same position , which were shown in Fig. 4(a).

Then the moisture related diffusion coefficient D(w) was obtained in terms of experimental results as illustrated in Eq. (19).

$$D(w) = -0.50931w^2 + 5.74369w - 4.98282 \quad (\times 10^{-6} m_2 / h) \tag{19}$$

Considering the effects of Knudsen diffusion(r = 0.09) and taking Eq. (19) in to Eq. (13), the effective diffusive coefficient was deduced as

$$D_{eff}(w) = -0.46347 \times 10^{-6} w^2 + 5.22676 \times 10^{-6} w - 4.70637 \times 10^{-6} \tag{20}$$

3.4.2 Other related calculation parameters

The other related calculation parameters were given in Table 3 for experimental concrete specimen that was initially seam and water cured.

3.5 Methods of numerical solutions

3.5.1 Mesh

The moisture transfer in concrete specimen with the length of 0.6m was obtained by solving the nonlinear diffusion-hydration Eq. (1). An implicit difference scheme was adopted to solve numerically the equation to obtain the water content distribution in the specimen with initially steam and water cuing. The discretization scheme was the specimen along the length of 0.6m was divided into many parts with the proportional spacing and the increment Δx. The discretization step of the time interval Δt was selected to describe the moisture transfer history induced by diffusion and hydration action. Thus the parallel lines are defined as $x_i = i\Delta x$ (i = 0, 1, 2…, i,…, M, M is the number of grid along the x direction), and $t_k = k\Delta t$ (k = 0, 1 , 2…, k ,…, M, M is the age of concrete specimen). Thus the moisture content at the state (x_i, t_k) could be expressed by w_i^k .

3.5.2 Finite difference scheme

Crank-Nicolson scheme (C-N scheme), which is relatively stable and convergent, was adopted to establish difference equation of Eq. (1). From the diagram of node of C-N scheme in Fig. (5) that $w_i^{k+1/2}$ was replaced by the average of w_i^{k+1} and w_i^k . Simultaneously nonlinear parameter $D_{eff}(w)$ was express by forward layer to establish linear scheme.

It was assumed that $\partial w_h / \partial t = g(t)$, D_{eff}(w) =$C_1w^2+C_2w+C_3$, h = 0.6/M and $\tau_w = t$/N. Thus the partial differential Eq. (1) could be replaced by the following difference quotients

$$\delta_t w_i^{n+1/2} = \frac{1}{\tau_w}(w_i^{n+1} - w_i^n) \tag{21}$$

$$w_{i+1/2} = \frac{1}{2}(w_i - w_{i+1)}) \tag{22}$$

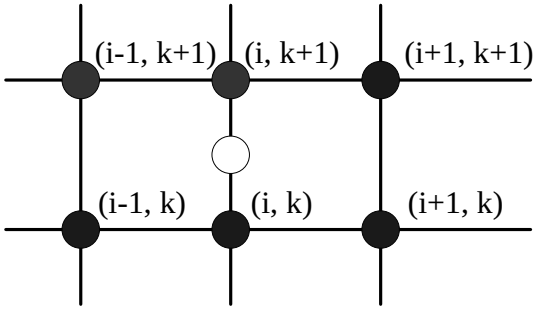

Fig. 5 Diagram of node for crank-nicolson mode

$$w_i^{n+1} = \frac{1}{2}(w_i^n - w_i^{n+1}) \tag{23}$$

$$D_{eff}(w_{i+1/2}^n) = C_1(w_{i+1/2}^n)^2 + C_2(w_{i+1/2}^n) + C_3 \tag{24}$$

$$\delta_t w_i^{n+1/2} = \frac{1}{h}\left[D_{eff}(w_{i+1/2}^n)\frac{w_{i+1}^{n+1/2} - w_i^{n+1/2}}{h} - D_{eff}(w_{i-1}^n)\frac{w_i^{n+1/2} - w_{i-1}^{n+1/2}}{h} \right] + g^{n+1/2} \quad \begin{matrix} 1 \le i \le M-1 \\ 0 \le n \le N-1 \end{matrix} \tag{25}$$

Substituting Eq. (21) ~ Eq. (25) into Eq. (1), and it was suggested that $s = \tau_w/h^2$, the finite difference with the C-N scheme of Eq. (1) at the intervals (t_k, t_{k+1}) could be expressed by

$$\begin{aligned}
&\left[-\frac{C_1 s}{2}\left(w_{i-1/2}^0\right)^2 - \frac{C_2 s}{2}\left(w_{i-1/2}^0\right) - \frac{C_3 s}{2} \right] w_{i-1}^n + \left[1 + \frac{C_1 s}{2}\left(w_{i+1/2}^0\right)^2 + \frac{C_1 s}{2}\left(w_{i-1/2}^0\right) + \frac{C_2 s}{2}\left(w_{i+1/2}^0 + w_{i-1/2}^0\right) + C_3 s \right] w_i^n + \\
&\left[-\frac{C_1 s}{2}\left(w_{i+1/2}^0\right) - \frac{C_2 s}{2} w_{i+1/2}^0 - \frac{C_3 s}{2} \right] w_{i+1}^n = \left[\frac{C_1 s}{2}\left(w_{i-1/2}^0\right) + \frac{C_2 s}{2}\left(w_{i-1/2}^0\right) + \frac{C_3 s}{2} \right] w_{i-1}^{n-1} + \\
&\left[1 - \frac{C_1 s}{2}\left((w_{i+1/2}^0)^2 + (w_{i-1/2}^0)^2\right) - \frac{C_2 s}{2}\left((w_{i+1/2}^0) + (w_{i-1/2}^0) - C_3 s\right) \right] w_i^{n-1} + \left[\frac{C_1 s}{2}(w_{i+1/2}^0)^2 + \frac{C_2 s}{2}(w_{i+1/2}^0) + \frac{C_3 s}{2} \right] w_{i+1}^{n-1} \\
&+ \tau \cdot g^{n+1/2}
\end{aligned} \tag{26}$$

As moisture content of every layer in Eq. (26) can be obtained by adopting chase method to solve one (M-1) - matrix tri-diagonal equations. It was notable that as numerical moisture content was lower than 80%, it was supposed that $g(t) = 0$. Therefore the moisture content at the point (x_i, t_k) was obtained by adopting the chase method to solve Eq. (26).

4. Verification and analysis of the numerical results

4.1 Comparison between experimental and model results

Using the model Eq. (1) and its C-N difference scheme the moisture content along the distance from drying surface was calculated, and the related parameters are shown in Table1-Table 3. The relation between water content and relative humidity was obtained according to the experimental methods in references (Kim 1999), which was shown in Fig. 6(a). The comparison of moisture

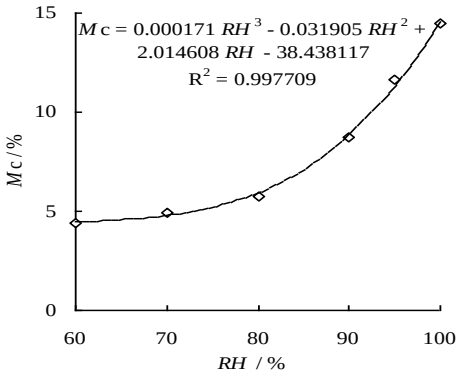

(a) The relation between relative humidity and water content

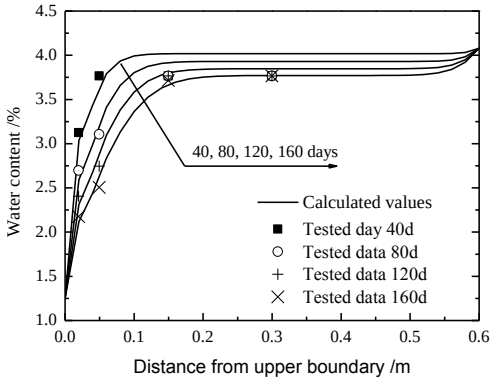

(b) experimental and calculated water content

Fig. 6 Comparison between calculated and experimental results of water content

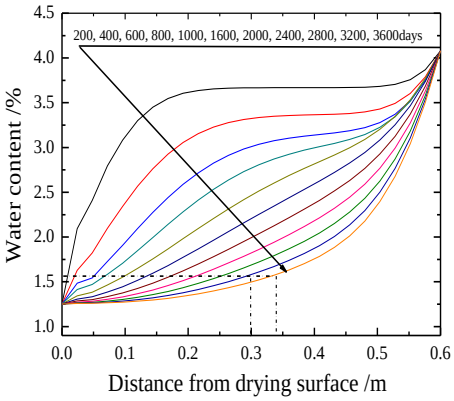

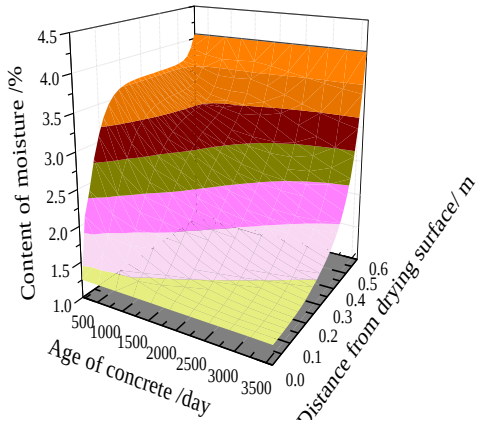

Fig. 7 Predicted values of water content varying with time and space

content between the model calculation and experimental results of concrete specimen at four ages was displayed by Fig. 6(b). The environmental humidity used in the calculation is the same as the humidity of the room where the testing of relative humidity were carried out.

It was seen from Fig. 6 that the numerical and experimental results agreed well with each other and the proposed model could catch the developing characteristics of moisture content inside concrete specimens. It was also observed that the moisture content near drying surface changed very quickly. The effects of water diffusion on moisture content transport at the nearer position from drying surface were much higher and the moisture content close to saturated soil was changed mainly by hydration force. From above figure, it could be seen that with increase of age the effects of hydration on moisture content change decreased.

Thus it could be concluded that the proposed model and solving method were reasonable to determine the moisture content development in concrete structures with large amounts of mineral admixtures, especially for concrete structures exposed to underwater condition in the relative early

age. Fig. 7 presented the predicted moisture content distribution in concrete segment for underwater tunnel.

From Fig. 7 it could be observed that the moisture gradients mainly distributed near the evaporable face of segment at early service ages and with the increase of service time the moisture gradients was promoted toward the saturation surface. This indicated that the water evaporation induced moisture gradients were the main cause for moisture diffusion at early age while the moisture gradient between saturation and evaporable surface are the main inducement at later service time. It could also be seen from Fig. 7 that moisture content at the 100 mm distance from evaporable surface reached equilibrium with environmental humidity condition at the age of 3600 days. Supposed 20 mm designed concrete cover of segment, the moisture content in its concrete cover achieved equilibrium with environmental condition at the age of 1600 days.

4.2 Discussion of model results

4.2.1 Effects of environmental humidity on moisture distribution

The drying surface of segment specimen is directly exposed to environmental humidity condition, so it was very necessary to consider the effects of environmental humidity on inner moisture distribution in segment specimen. Fig. 8 showed the moisture distribution along the segment specimen exposed to 50%, 70% and 90% relative humidity at the age of 800 days.

It could be seen from Fig.8 that the environmental humidity had more influence on the moisture distribution near the exposed specimen surface while the moisture content far from the dry surface was seldom affected. With the increase of environmental humidity condition, the inner moisture gradient decreased obviously.

4.2.2 Effects of per-cubic cement content on moisture distribution

As the hydration of cement induced water loss of segment concrete at early age, the cement content in per-cubic concrete segment inevitably exhibited certain influence on moisture distribution of segment concrete. Fig. 9 illustrated the moisture distribution of concrete segment with different per-cubic cement content at the age of 120 days and 600 days respectively.

It could be observed from Fig. 8 that the per-cubic cement content exerted obvious influence on moisture distribution of segment specimen. With increase of cement content, the moisture content decreased obviously along the segment specimen. It could also been seen from Fig.9 that the cement content had wide influencing range on segment specimen at more earlier ages and with the increase of hydration age the per-cubic cement content exerted very light effects on moisture content distribution of segment specimen.

4.2.3 Effects of capillary porosity on moisture distribution of segment specimen

The evaporable water is composed of capillary water and the capillary porosity at the surface exposed to saturated soil was supposed to be the corresponding moisture content of segment specimen. Thus the capillary porosity must have great influence on moisture content distribution of segment. Fig. 10 presented the calculated moisture content distribution of segment specimen with different capillary porosity.

It could be deduced from Fig. 10 that the segment specimen with smaller capillary porosity exhibited lower moisture content and had great moisture gradient near the saturated surface. While the segment with larger capillary porosity illustrated larger moisture gradients near the drying surface.

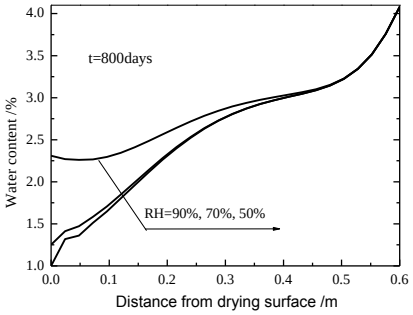

Fig. 8 Moisture content in segment specimen with different environmental humidity condition

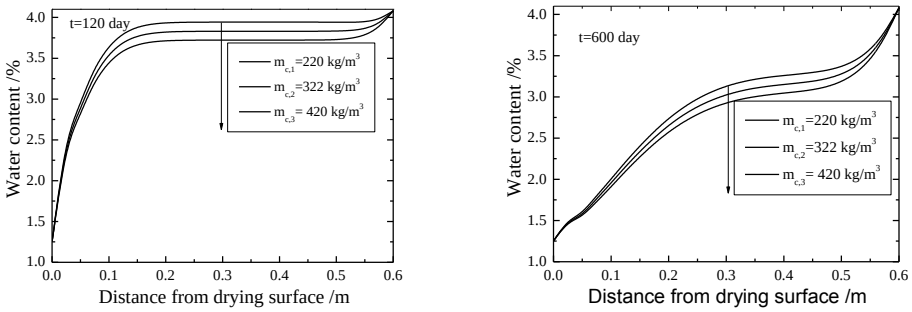

Fig. 9 Effects of cement content in per-cubic concrete on moisture distribution

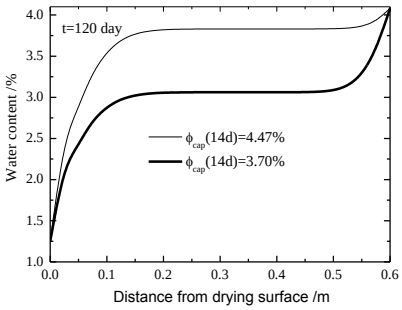

Fig.10 Numerical results of water content distribution varying with capillary porosity

5. Conclusions

(1) Experimental results of moisture distribution along simulated segment specimen showed that the relative humidity in outer layer near the drying surface decreased very quickly and achieved equilibrium with environmental humidity.

(2) A nonlinear moisture transport model considering diffusion, hydration and permeability was proposed. The moisture diffusion coefficient relating to moisture content and Knudsen diffusion

was determined by combining experimental and calculation results.

(3) The finite differential method was adopted to calculate the moisture distribution along segment specimen by linearizing the nonlinear moisture diffusion coefficient. The comparison between experimental and calculating results showed that the proposed moisture distribution model could be used to well predict the moisture content distribution inside underground concrete.

Acknowledgements

The authors are highly appreciated the financial support from the National Natural Science Foundation of China (51308308), the project supported by the Natural Science Foundation of Zhejiang Province (LQ12E08002), the Natural Science Foundation of Ningbo City (2012A610159), Ministry of Housing Project (2012-K4-7), Shandong Province Postdoctoral Innovation Project (201203023) and the project supported by K.C Wong Magna Fund in Ningbo University.

References

Breugela, K.V. and Koendersb, E.A.B. (2000), "Numerical simulation of hydration-driven moisture transport in bulk and interface paste in hardening concrete", *Cement Concrete. Res.*, **30**(5), 1911-1914.

Buffo-Lacarrière, L., Sellier, A., Escadeillas, G. and Turatsinze, A. (2007), "Multiphasic finite element modeling of concrete hydration", *Cement Concrete. Res.*, **37**(2), 131-138.

Fraj, A.F., Bonnet, S. and Khelidj, A. (2012), "New approach for coupled chloride/moisture transport in non-saturated concrete with and without slag", *Constr. Build. Mater.*, **35**, 761-771.

Garboczi, E.J.D. and Bentz, P. (1996), "Modeling of the microstructure and transport", *Constr. Build. Mater.*, **10**(5), 293-300.

Khelidj, A., Bastian, G., Baroghel-Bouny, V. and Villain, G. (2007), "Experimental study of the evolution of heat and moisture transfer parameters of a concrete slab", *Mag. Concr. Res.*, **59**(5), 377-386.

Krstulovic, R. and Dabic, P.A. (2000), "Conceptual model of the cement hydration process", *Cement. Concrete. Res.*, **30**(5), 693-698.

Knudsen, T. (1984), "The dispersion model for hydration of portland cement I. general concepts", *Cement Concrete. Res.*, **14**(6), 22-30.

Kim, J.K. and Lee, C.S. (1999), "Moisture diffusion of concrete considering self-desiccation at early ages", *Cement Concrete Res.*, **29**(12), 1921-1927.

Nilsson, L.O. (2002), "Long-term moisture transport in high performance concrete", *Mater. Struct.*, **35**(254), 641-649.

Oh, B.H. and Cha, S.W. (2003), "Nonlinear analysis of temperature and moisture distributions in early-age concrete structures based on degree of hydration", *ACI. Mater. J.*, **100**(5), 361-370.

Parrott, L.J. (1995), "Influence of cement type and curing on the drying and air permeability of cover concrete", *Mag. Concrete. Res.*, **47**(171), 103-111.

Ozbolt, J., Balabanic, G., Periskic, G. and Kuster, M. (2010), "Modeling the effect of damage on transport processes in concrete", *Constr. Build. Mater*, **24**(9), 1638-1648.

Powers, T.C. (1947), "A discussion of cement hydration in relation to the curing of concrete", *Research and Development Laboratoryes of the Portland Cement Association, Bulletin 25, Proceedings of the highway research board.*, **27**, 178-188.

Papadakis, V.G. (1999), "Effect of fly ash on Portland cement systems Part I. Low-calcium fly ash", *Cement Concrete Res.*, **29**(11), 1727-1736.

Qin, M., Belarbi, R., Ait-Mokhtar, A. and Nilsson, L.O. (2009), "Coupled heat and moisturetransfer in multi-layer building materials", *Constr. Build. Mater*, **23**(2), 967-975.

Qian, C.X., Wang, Y.J. and Huang, B. (2009), "Sewage law of water in concrete", *J. Constr. Mater.*, **5**(12), 515-518.

Tariku, F., Kumaran, K. and Fazio. P. (2010), "Transient model for coupled heat, air and moisture transfer through multilayered porous media", *Int. J. Heat Mass Transf.*, **53**(15-16), 3035-3044.

Wang, X.Y. and Lee, H.S. (2010), "Modeling the hydration of concrete incorporating fly ash or slag", *Cement Concrete Res.*, **40**(7), 984-996.

Ye, G. (2005), "Percolation of capillary pores in hardening cement pastes", *Cement. Concrete Res*, **35**, 167-176.

Zhang, J., Qi, K. and Huang, Y. (2009), "Calculation of moisture distribution in early-age concrete", *J. Eng. Mech.*, **13**5(8), 871-880.

CC